nature

https://doi.org/10.1038/s41586-020-2381-y

Accelerated Article Preview

A human neutralizing antibody targets the receptor binding site of SARS-CoV-2

Received: 2 April 2020

Accepted: 19 May 2020

Accelerated Article Preview Published online 26 May 2020

Cite this article as: Shi, R. et al. A human neutralizing antibody targets the receptor binding site of SARS-CoV-2. *Nature* https://doi.org/10.1038/s41586-020-2381-y (2020).

Rui Shi, Chao Shan, Xiaomin Duan, Zhihai Chen, Peipei Liu, Jinwen Song, Tao Song, Xiaoshan Bi, Chao Han, Lianao Wu, Ge Gao, Xue Hu, Yanan Zhang, Zhou Tong, Weijin Huang, William Jun Liu, Guizhen Wu, Bo Zhang, Lan Wang, Jianxun Qi, Hui Feng, Fu-sheng Wang, Qihui Wang, George Fu Gao, Zhiming Yuan & Jinghua Yan

Article

A human neutralizing antibody targets the receptor binding site of SARS-CoV-2

https://doi.org/10.1038/s41586-020-2381-y

Received: 2 April 2020

Accepted: 19 May 2020

Published online: 26 May 2020

Rui Shi[1,2,14], Chao Shan[3,14], Xiaomin Duan[1,2,14], Zhihai Chen[4,14], Peipei Liu[5,14], Jinwen Song[6,14], Tao Song[1,7,8], Xiaoshan Bi[1,9], Chao Han[1,2], Lianao Wu[9,10], Ge Gao[3], Xue Hu[3], Yanan Zhang[3], Zhou Tong[1,10], Weijin Huang[11], William Jun Liu[5], Guizhen Wu[5], Bo Zhang[3], Lan Wang[11], Jianxun Qi[10,12], Hui Feng[13], Fu-sheng Wang[6]✉, Qihui Wang[1,10]✉, George Fu Gao[10]✉, Zhiming Yuan[3]✉ & Jinghua Yan[1,10,12]✉

An outbreak of the coronavirus disease 2019 (COVID-19)[1–3], caused by the severe acute respiratory syndrome coronavirus 2 (SARS-CoV-2)[4] spread globally. Countermeasures are needed to treat and prevent further dissemination of the virus. In this study, we report the isolation of 2 specific human monoclonal antibodies (MAbs) from a convalescent COVID-19 patient. CA1 and CB6 demonstrated potent SARS-CoV-2-specific neutralization activity *in vitro* against SARS-CoV-2. In addition, CB6 inhibited SARS-CoV-2 infection in rhesus monkeys at both prophylactic and treatment settings. Further structural studies revealed that CB6 recognizes an epitope that overlaps with angiotensin converting enzyme 2 (ACE2)-binding sites in SARS-CoV-2 receptor binding domain (RBD), thereby interfering with the virus/receptor interactions by both steric hindrance and direct interface-residue competition. Our results suggest CB6 deserves further clinical translation.

Emerging and recurrent pathogens are global challenges for public health[5]. Since the end of 2019, cases of atypical pneumonia, now officially designated as coronavirus disease 2019 (COVID-19) by World Health Organization (WHO), has been reported[1–3]. The underlying pathogen was later confirmed to be a novel coronavirus (CoV), which is closely related to a bat CoV based on phylogeny[6]. Recently, the International Committee on Taxonomy of Viruses (ICTV) named the virus as SARS-CoV-2[4], although many virologists argue that HCoV-19 is more appropriate[7]. As of April 1st, there were over 880,000 confirmed cases, and over 44,000-related death globally (https://www.who.int/). No vaccines or drugs have been approved for the treatment of COVID-19. However, multiple clinical trials have been launched to evaluate the efficacy and safety of inactivated convalescent plasma in the treatment of COVID-19 (https://clinicaltrials.gov/). The preliminary data revealed potential benefit from convalescent plasma treatment (http://www.nhc.gov.cn/), indicating neutralizing antibodies from convalescent patients could inhibit virus infection and have potentials for clinical usage. However, the practical limitations of convalescent plasma collection and lack of suitable risk assessment make large-scale convalescent plasma transfusion program a challenge.

SARS-CoV-2 represents the third emerged highly pathogenic CoVs infecting humans and it uses the same receptor angiotensin converting enzyme 2 (ACE2) for cell entry as severe acute respiratory syndrome coronavirus (SARS-CoV)[6,8]. As with other CoVs, the SARS-CoV-2 Spike protein (S protein) would be further cleaved into S1 and S2 subdomains, with S1 binding to host receptor and S2 mediating membrane fusion[9]. Recently, we and other researchers mapped the receptor binding domain (RBD) in SARS-CoV-2 S protein at S1 C-terminal domain (CTD) and solved the crystal structure of SARS-CoV-2-RBD in complex with human ACE2 (hACE2)[10–13][REMOVED HYPERLINK FIELD]. Previous studies revealed that a large number of antibodies showed neutralization activity by targeting the RBD of either SARS-CoV or Middle East respiratory syndrome coronavirus (MERS-CoV) presumably by disrupting the virus-receptor engagement[14–16]. Thus, we attempted to isolate neutralizing monoclonal antibodies (MAbs) against SARS-CoV-2 from convalescent patients, using a similar strategy previously reported[17,18].

We utilized recombinant RBD of SARS-CoV-2 S protein as the bait to sort specific memory B cells from peripheral blood mononuclear cells (PBMCs) of a COVID-19 convalescent patient. The sequences of the variable regions of IgG antibodies in the sorted cells were obtained through 5' RACE amplification from individual B cell. Two MAbs, named CA1 and CB6 (Extended Data Table 1), were identified to be able to block the binding of soluble SARS-CoV-2-RBD with hACE2 receptor transiently expressed on HEK293T cells (Fig. 1a). Binding analysis of CA1 and CB6 by flow cytometry (FACS) revealed that both MAbs could specifically bind to SARS-CoV-2 S protein transfected HEK293T cells, but not SARS-CoV

[1]CAS Key Laboratory of Microbial Physiological and Metabolic Engineering, Institute of Microbiology, Chinese Academy of Sciences, Beijing, 100101, China. [2]University of Chinese Academy of Sciences, Beijing, 100049, China. [3]Center for Biosafety Mega-Science, Wuhan Institute of Virology, Chinese Academy of Sciences, Wuhan, Hubei, 430071, China. [4]Center of Infectious Disease, Beijing Ditan Hospital, Capital Medical University, Beijing, 100015, China. [5]NHC Key Laboratory of Biosafety, National Institute for Viral Disease Control and Prevention, Chinese Center for Disease Control and Prevention, Beijing, 102206, China. [6]Treatment and Research Center for Infectious Diseases, The Fifth Medical Center of PLA General Hospital, National Clinical Research Center for Infectious Diseases, Beijing, 100039, China. [7]Shanxi Academy of Advanced Research and Innovation, Taiyuan, 030032, China. [8]College of Animal Science and Technology, Hebei Normal University of S&T, Qinhuangdao, 066004, China. [9]Institute of Physical Science and Information, Anhui University, Hefei, 230039, China. [10]CAS Key Laboratory of Pathogenic Microbiology and Immunology, Institute of Microbiology, Chinese Academy of Sciences, Beijing, 100101, China. [11]Key Laboratory of the Ministry of Health for Research on Quality and Standardization of Biotech Products, National Institutes for Food and Drug Control, Beijing, 100050, China. [12]Savaid Medical School, University of Chinese Academy of Sciences, Beijing, 100049, China. [13]Shanghai Junshi Biosciences Co., Ltd, Shanghai, 201203, China. [14]These authors contributed equally: Rui Shi, Chao Shan, Xiaomin Duan, Zhihai Chen, Peipei Liu, Jinwen Song. ✉e-mail: fswang302@163.com; wangqihui@im.ac.cn; gaof@im.ac.cn; yzm@wh.iov.cn; yanjh@im.ac.cn

S or MERS-CoV S transfected cells (Fig. 1b). The binding kinetics of CA1 and CB6 were assessed by a surface plasmon resonance (SPR) assay. The measured equilibrium constant (K_D) of CA1 and CB6 with SARS-CoV-2-RBD were 4.68 ± 1.64 nM and 2.49 ± 1.65 nM, respectively (Fig. 1c and Extended Data Table 2). As CA1 and CB6 have distinctive CDR sequences (Extended Data Table 1), we examined the potential competitive binding of CA1 and CB6 to SARS-CoV-2-RBD in an Octet based binding assay. Recombinant SARS-CoV-2-RBD protein was first biotinylated and immobilized on a streptavidin biosensor and then saturated with CB6 or CA1. Addition of CA1 to CB6 saturated probe or CB6 to CA1 saturated probe showed no complementary binding (Extended Data Fig. 1), indicating CA1 and CB6 bind to overlapped epitopes on SARS-CoV-2-RBD.

The neutralization abilities of CA1 and CB6 against SARS-CoV-2 infection was first investigated using pseudoviruses expressing S antigen of SARS-CoV-2 and then live virus *in vitro*. Both CA1 and CB6 inhibit pseudovirus transduction into Huh7 cells, Calu-3 and HEK293T cells (Fig. 2a, c). Notably, CB6 had stronger neutralizing activity than CA1 in terms of 50% neutralization dose (ND_{50}) in all three tested cell lines. Consistently, CB6 also exhibited stronger neutralizing activity than CA1 against live SARS-CoV-2 infection of Vero E6 cells, with observed ND_{50} of 0.036 ± 0.007 μg/mL for CB6 and 0.38 μg/mL for CA1 (Fig. 2d, e). In summary, both MAbs exhibit substantial neutralizing activities against SARS-CoV-2 infection *in vitro*, while CB6 exhibited superior neutralizing activity over CA1.

The CB6 MAb was further tested *in vivo* in rhesus macaque SARS-CoV-2 infection model[REMOVED HYPERLINK FIELD] at both prophylactic and treatment settings. Given the potential risk of antibody-dependent enhancement (ADE) effect as observed in SARS-CoV infection[19,20], we introduced the LALA mutation to the Fc portion of CB6 (CB6-LALA) to lower the risk of Fc-mediated acute lung injury. In the treatment group, three animals (6-8 years old) were challenged with 1×10^5 50% tissue culture infectious dose ($TCID_{50}$) SARS-CoV-2 via intratracheal incubation. CB6-LALA (50 mg/kg) was administered at days 1 and 3 post infection (dpi) intraperitoneally. Animals in the control group (n=3) were given an equal volume of phosphate-buffered saline (PBS) on both 1 and 3 dpi. The viral titers from throat swabs were evaluated daily till 7 dpi. In the control group, the viral loads reached peak levels (approximately $10^{6.5}$ RNA copies/mL) on 4 dpi and then declined naturally (Fig. 3a). In contrast, CB6-LALA treatment reduced virus titers immediately after administration. Specifically, on 4 dpi, CB6-LALA reduced the viral titer by an approximately 3 logs than that of the control group (Fig. 3a). Additionally, in the prophylactic group of three animals, a single dose of CB6-LALA (50 mg/kg) before SARS-CoV-2 challenge significantly protected the animal from SARS-CoV-2 infection. Only minimal levels of virus were detected in the throat swabs in this group and the peak viral load was no more than 10^3 RNA copies/mL (Fig. 3a), indicating a strong prophylactic protection effect of CB6-LALA antibody against SARS-CoV-2 infection.

In addition to viral titer reduction, we further investigated whether CB6-LALA also inhibited the pathological lung damage in the monkeys challenged with SARS-CoV-2. One monkey from each group was euthanized and necropsied on 5 dpi. Control animal displayed interstitial pneumonia characterized by thickened alveolar septa, proliferation and fibrosis of fibroblasts, with intensive infiltration of monocytes and lymphocytes cells. In some alveolar cavities, cellulose exudation could be observed, with the formation of hyaline membrane and pulmonary hemorrhage. There was also clear thrombosis in the pulmonary capillary lumen, with accumulation of necrotic and exfoliated epithelial cells of the bronchioles (Fig. 3b). In contrast, monkeys treated prophylactically or post infection displayed limited pathological lung damages. Either monkey in the treatment group or prophylactic group had overall intact alveolar structure, reduced edema, and no formation of hyaline membrane, with significantly less fibrosis and less leukocyte infiltrations as compared with the control animals (Fig. 3c, d). In addition, no serious small bronchi and pulmonary capillary lesions were observed (Fig. 3c, d). Thus, CB6-LALA could inhibit SARS-CoV-2 viral titer and reduce infection-related lung damage, at both prophylactic and treatment settings.

To further investigate the blocking and neutralizing mechanisms of CB6, protein complex of recombinant CB6-Fab/SARS-CoV-2-RBD proteins were prepared for crystal screening (Extended Data Fig. 2). The 3-D structure of CB6-Fab/SARS-CoV-2-RBD complex was determined by X-ray crystallography at an overall resolution of 2.9 Å (Extended Data Table 3). Overall, CB6 binds to SARS-CoV-2-RBD with a buried surface of 1088 $Å^2$ (Fig. 4a). Specifically, the CB6 V_H dominates the interaction with SARS-CoV-2-RBD by all the three CDRs, forming concentrated polar contacts (Fig. 4b and Extended Data Table 4) and hydrophobic interactions (Fig. 4c and Extended Data Table 4). While V_L has limited contacts with LCDR1 and LCDR3 loop (Fig. 4d and Extended Data Table 4).

To analyze the blocking mechanisms of CB6 to SARS-CoV-2-RBD/hACE2 interaction, the complex structure of CB6-Fab/SARS-CoV-2-RBD was superimposed with hACE2/SARS-CoV-2-RBD complex (PDB: 6LZG) (Fig. 4e). Superimposition of the RBD in its CB6-bound form with its hACE2-bound form resulted in Cα root mean squared deviation (RMSD) of 0.282 Å (for 169 atoms), indicating that binding of CB6 did not induce significant conformational changes in SARS-CoV-2-RBD. The binding of CB6 has induced steric hindrance to the binding of hACE2, which is mediated by both V_H and V_L of CB6 (Fig. 4e). The whole CB6 light chain, as well as most of the heavy chain have structure clashes with the receptor. There are also substantial overlapped binding areas between CB6 and hACE2 on RBD (Fig. 4f). In summary, the blocking mechanisms of CB6 depends on both of its V_H and V_L which provides steric hindrance and direct interface-residue competition to abrogate the binding of hACE2 to SARS-CoV-2-RBD.

Previous studies focusing on SARS-CoV infection *in vitro* and in mouse models[19,20] indicate the potential risk of ADE hindering the ability of antibody therapeutics to control inflammation in the lung and other organs. On the contrary, ADE may lead to acute respiratory injury, acute respiratory distress syndrome, and other observed inflammation-based sequelae. Given the highly phylogenetic relationship between SARS-CoV and SARS-CoV-2, the risk of ADE needs to be mitigated. To solve this problem, we introduced the LALA mutations to the Fc portion of CB6 molecule to eliminate ADCC effect. Subsequently, CB6-LALA showed protective effect in rhesus monkey infection model and did not exacerbate tissue damage induced by the infection. To our knowledge, this represents the first report to evaluate the function of neutralizing MAbs against SARS-CoV-2 using nonhuman primates and would shed light on the design of dosing regimen in clinical trials.

Currently, no approved drugs or vaccines have been approved against COVID-19, highlighting the great unmet medical needs to develop therapeutics. Neutralizing MAbs are promising candidates to combat emerging viruses. Using Ebola virus as an example, ZMapp save two Americans in 2014[21] and MAb114 had shown striking treatment benefits, reducing the mortality rate of Ebola virus disease from ~67% to 34% for all patients and 9.9% for patients with low viral loads[22]. Recently, MAb114 was granted breakthrough therapy designation for the treatment of Ebola virus disease. The neutralizing activity *in vitro* and protection efficacy *in vivo* of CB6 against SARS-CoV-2 is good and is likely to be comparable to MAb114 against Ebola virus[23,24].

In addition to the post-exposure treatment, neutralizing MAbs can also be used at prophylactic setting. The first FDA-approved MAbs against infectious diseases is palivizumab, which is indicated for the prophylaxis of preterm infants and children at high-risk for respiratory syncytia virus (RSV) infections. The pandemic of SARS-CoV-2 poses great risks to front line health care workers, elderly patients, and patients with pre-existing conditions. At the current situation when vaccines are not available, any preventative treatments are greatly needed. Our *in vivo* protection data at pre-exposure settings indicated that CB6 is a promising candidate as a prophylaxis for COVID-19.

Structural analysis revealed the molecular basis for the neutralizing activity of CB6 MAb. Notably, the interacting epitopes on SARS-CoV-2-RBD for CB6 are highly overlapped with the binding epitopes of hACE2, indicating a strong resistance potential to SARS-CoV-2 mutation variants. Based on the available 157 SARS-CoV-2 viral genomes deposited in NCBI databank as of April 1st, 2020, two substitutions in the RBD region were observed, namely G476S and V483A (Extended Data Fig. 3). Although G476S locates in the binding interface with CB6 MAb, this residue has limited contribution to the antibody-antigen interaction and is thus unlikely influence the binding of CB6.

During the revision of this manuscript, CR3022, a neutralizing antibody against SARS-CoV previously isolated from a convalescent SARS patient, was found to be cross-reactive with SARS-CoV-2-RBD. Crystal structure analysis revealed that CR3022 targets a highly conserved epitope, distal from the receptor-binding site and does not neutralize SARS-CoV-2 infection[25]. Superimposition of the SARS-CoV-2-RBD in complex with either CB6 or CR3022 (PDB: 6W41) indicated that CB6 will unlikely exert any effect on the binding of CR3022 and vice versa (Extended Data Fig. 4). Nevertheless, the reported molecular basis for the binding of CR3022 with SARS-CoV-2-RBD deepened our understanding of antibody recognition of SARS-CoV-2.

In conclusion, our data indicated CB6, a neutralizing MAb isolated from a convalescent COVID-19 patient, could be a potential therapeutic agent for COVID-19 and deserves further translational development.

Online content

Any methods, additional references, Nature Research reporting summaries, source data, extended data, supplementary information, acknowledgements, peer review information; details of author contributions and competing interests; and statements of data and code availability are available at https://doi.org/10.1038/s41586-020-2381-y.

1. Tan, W. *et al*. Notes from the field: A novel coronavirus genome identified in a cluster of pneumonia cases - Wuhan, China 2019-2020. *China CDC Weekly* **2**, 61-62 (2020).
2. The 2019-nCoV Outbreak Joint Field Epidemiology Investigation Team & Li, Q. Notes from the field: An outbreak of NCIP (2019-nCoV) infection in China - Wuhan, Hubei province, 2019-2020. *China CDC Weekly* **2**, 79-80 (2020).
3. Wang, C., Horby, P. W., Hayden, F. G. & Gao, G. F. A novel coronavirus outbreak of global health concern. *Lancet*, https://doi.org/10.1016/S0140-6736(20)30185-9 (2020).
4. ICTV, C. S. G. O. T. The species Severe acute respiratory syndrome-related coronavirus: classifying 2019-nCoV and naming it SARS-CoV-2. *Nat Microbiol*, https://doi.org/10.1038/s41564-020-0695-z (2020).
5. Gao, G. F. From "A"IV to "Z"IKV: Attacks from emerging and re-emerging pathogens. *Cell* **172**, 1157-1159, https://doi.org/10.1016/j.cell.2018.02.025 (2018).
6. Zhou, P. *et al*. A pneumonia outbreak associated with a new coronavirus of probable bat origin. *Nature*, https://doi.org/10.1038/s41586-020-2012-7 (2020).
7. Jiang, S. *et al*. A distinct name is needed for the new coronavirus. *The Lancet*, https://doi.org/10.1016/S0140-6736(20)30419-0 (2020).
8. Hoffmann, M. *et al*. SARS-CoV-2 cell entry depends on ACE2 and TMPRSS2 and is blocked by a clinically proven protease inhibitor. *Cell*, https://doi.org/10.1016/j.cell.2020.02.052 (2020).
9. Lu, G., Wang, Q. & Gao, G. F. Bat-to-human: spike features determining 'host jump' of coronaviruses SARS-CoV, MERS-CoV, and beyond. *Trends Microbiol* **23**, 468-478, https://doi.org/10.1016/j.tim.2015.06.003 (2015).
10. Wang, Q. *et al*. Structural and functional basis of SARS-CoV-2 entry by using human ACE2. *Cell*, https://doi.org/10.1016/j.cell.2020.03.045 (2020).
11. Shang, J. *et al*. Structural basis of receptor recognition by SARS-CoV-2. *Nature*, https://doi.org/10.1038/s41586-020-2179-y (2020).
12. Lan, J. *et al*. Structure of the SARS-CoV-2 spike receptor-binding domain bound to the ACE2 receptor. *Nature*, https://doi.org/10.1038/s41586-020-2180-5 (2020).
13. Yan, R. *et al*. Structural basis for the recognition of the SARS-CoV-2 by full-length human ACE2. *Science*, https://doi.org/10.1126/science.abb2762 (2020).
14. Li, Y. *et al*. A humanized neutralizing antibody against MERS-CoV targeting the receptor-binding domain of the spike protein. *Cell Res* **25**, 1237-1249, https://doi.org/10.1038/cr.2015.113 (2015).
15. Du, L. Y. *et al*. The spike protein of SARS-CoV - a target for vaccine and therapeutic development. *Nat Rev Microbiol* **7**, 226-236, https://doi.org/10.1038/nrmicro2090 (2009).
16. Wang, Q., Wong, G., Lu, G., Yan, J. & Gao, G. F. MERS-CoV spike protein: Targets for vaccines and therapeutics. *Antiviral Res* **133**, 165-177, https://doi.org/10.1016/j.antiviral.2016.07.015 (2016).
17. Wang, Q. *et al*. Molecular determinants of human neutralizing antibodies isolated from a patient infected with Zika virus. *Sci Transl Med* **8**, 369ra179, https://doi.org/10.1126/scitranslmed.aai8336 (2016).
18. Wang, Q. *et al*. Neutralization mechanism of human monoclonal antibodies against Rift Valley fever virus. *Nat Microbiol* **4**, 1231-1241, https://doi.org/10.1038/s41564-019-0411-z (2019).
19. Channappanavar, R. *et al*. Dysregulated Type I Interferon and Inflammatory Monocyte-Macrophage Responses Cause Lethal Pneumonia in SARS-CoV-Infected Mice. *Cell Host Microbe* **19**, 181-193, https://doi.org/10.1016/j.chom.2016.01.007 (2016).
20. Liu, L. *et al*. Anti–spike IgG causes severe acute lung injury by skewing macrophage responses during acute SARS-CoV infection. *JCI Insight* **4**, https://doi.org/10.1172/jci.insight.123158 (2019).
21. Lyon, G. M. *et al*. Clinical care of two patients with Ebola virus disease in the United States. *N Engl J Med* **371**, 2402-2409, https://doi.org/10.1056/NEJMoa1409838 (2014).
22. Mulangu, S. *et al*. A randomized, controlled trial of Ebola virus disease therapeutics. *N Engl J Med* **381**, 2293-2303, https://doi.org/10.1056/NEJMoa1910993 (2019).
23. Gaudinski, M. R. *et al*. Safety, tolerability, pharmacokinetics, and immunogenicity of the therapeutic monoclonal antibody mAb114 targeting Ebola virus glycoprotein (VRC 608): an open-label phase 1 study. *Lancet* **393**, 889-898, https://doi.org/10.1016/S0140-6736(19)30036-4 (2019).
24. Corti, D. *et al*. Protective monotherapy against lethal Ebola virus infection by a potently neutralizing antibody. *Science* **351**, 1339-1342, https://doi.org/10.1126/science.aad5224 (2016).
25. Yuan, M. *et al*. A highly conserved cryptic epitope in the receptor-binding domains of SARS-CoV-2 and SARS-CoV. *Science*, eabb7269, https://doi.org/10.1126/science.abb7269 (2020).
26. Sui, J. *et al*. Potent neutralization of severe acute respiratory syndrome (SARS) coronavirus by a human mAb to S1 protein that blocks receptor association. *Proceedings of the National Academy of Sciences of the United States of America* **101**, 2536-2541, https://doi.org/10.1073/pnas.0307140101 (2004).

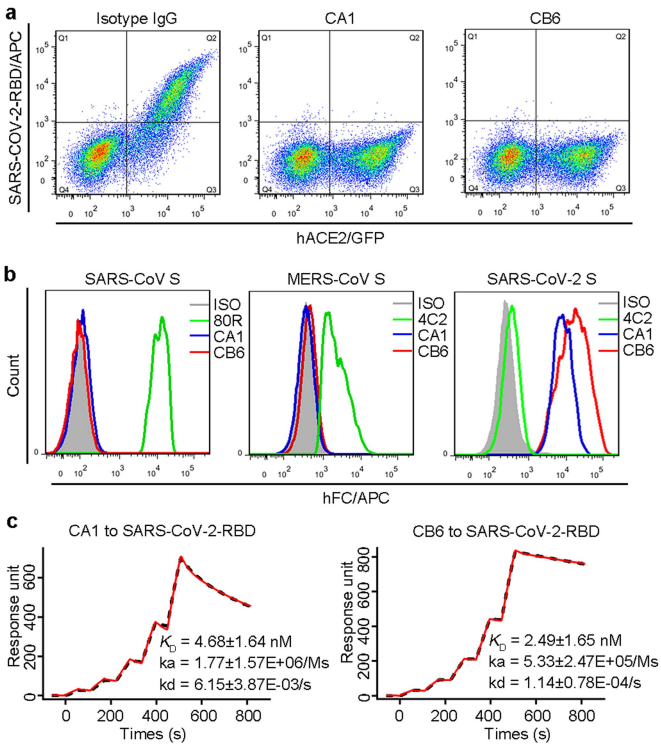

Fig. 1 | MAb CA1 and CB6 specifically recognize RBD and block binding of SARS-CoV-2-RBD to hACE2 receptor. a, CA1 and CB6 can block SARS-CoV-2-RBD binding to hACE2 in FACS-based assay. hACE2-GFP fusion protein was transiently expressed on HEK293T cell surface, and stained with SARS-CoV-2-RBD proteins pre-incubated with isotype control IgG, CA1 or CB6. Experiments were performed twice and one representative data were displayed. **b**, HEK293T cells expressing SARS-CoV S were permeabilized, and stained with isotype control IgG, CA1, CB6 or positive control MAb 80R[26]. Cells with MERS-CoV S and SARS-CoV-2 S were stained with isotype control IgG, CA1, CB6 or control MAb 4C2[14]. Experiments were performed twice and one representative data were displayed. **c**, The binding kinetics of CA1 and CB6 to recombinant SARS-CoV-2-RBD protein were obtained using BIAcore 8K system with a single-cycle mode. MAbs were captured on the chip while serial dilutions of RBD proteins were then injected over the chip surface. The K_D was labeled accordingly. Values represented Mean ± SD of three independent results.

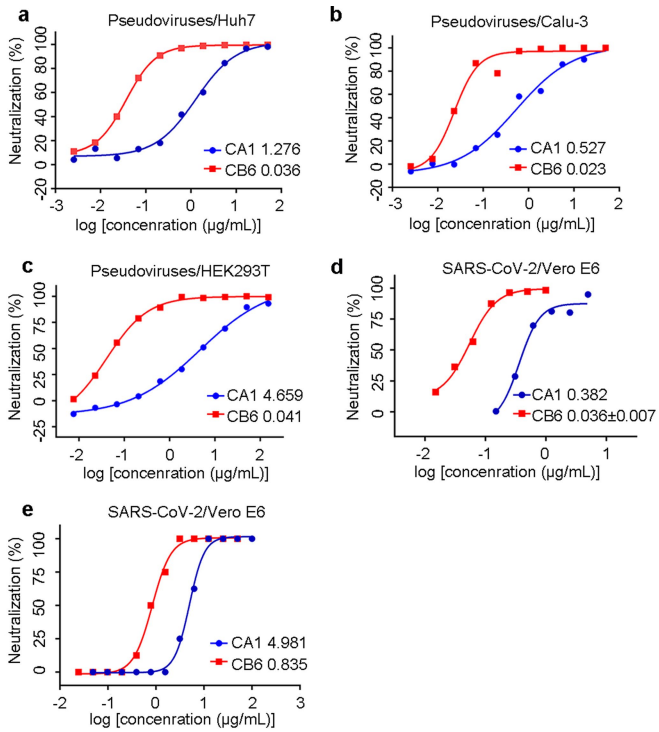

Fig. 2 | CB6 and CA1 can effectively neutralize SARS-CoV-2 pseudovirus or live SARS-CoV-2 virus *in vitro*. a-c, SARS-CoV-2 pseudovirus were incubated with 3-fold serially diluted CA1 or CB6. The mixtures were then added to Huh7 (a), Calu-3 (b) or HEK293T cells (c). After 24 h incubation, neutralizations potencies of MAbs were evaluated in a luciferase assay system. ND_{50} was calculated by fitting the luciferase activity from serially diluted antibody to a sigmoidal dose-response curve. The experiments were performed twice and similar results were obtained. One representative data of one experiment were shown and data were average values of two replicates. **d**, The mixtures of live SARS-CoV-2 virus and serially diluted CA1 or CB6 were added to Vero E6 cells. After 30 h incubation, ND_{50} was calculated by fitting the viral RNA copies (determined by qRT-PCR) from serially diluted antibody to a sigmoidal dose-response curve. The experiments for CA1 were performed twice and similar results were obtained. For CB6, the values shown are the mean ± SD of three independent experiments. For both CA1 and CB6, one representative data of one experiment were shown and data were average values of two replicates. **e**, The mixtures of SARS-CoV-2 and serially diluted CA1 or CB6 were added to Vero E6 cells. After 72 h incubation, ND_{50} were calculated by fitting the proportion of CPE with serially diluted antibody to a sigmoidal dose-response curve. The experiments were independently performed twice and similar results were obtained. One representative data were shown.

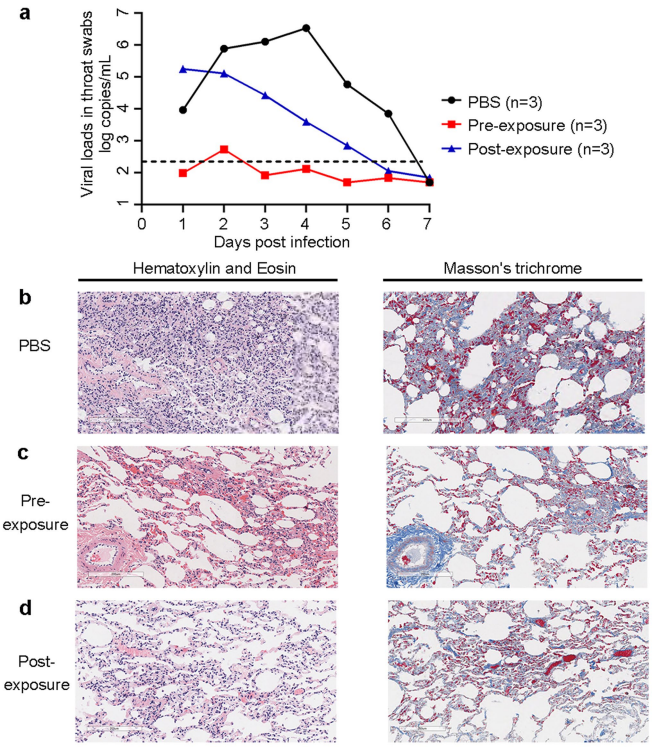

Fig. 3 | CB6 MAb can effectively reduce viral load and alleviated infection-related lung damage in rhesus macaques. a, Nine male rhesus macaques were divided into pre-challenge (prophylactic), post-challenge (treatment) and control groups with 3 animals in each group. Before infection, the animals of pre-challenge group were infused with 50 mg/kg CB6-LALA intravenously. One day later, all macaques were inoculated with 1×10^5 $TCID_{50}$ SARS-CoV-2 via intratracheal intubation. While the post-challenge group were also infused with 50 mg/kg antibody CB6-LALA on days 1 and 3 post challenge and three monkeys in the control group were given PBS as a control. Viral RNA loads in throat swabs determined by qRT-PCR were monitored for 7 days. Data were average values from three monkeys (n=3) for the first 5 days, from two monkeys (n=2) for the 6 dpi, and from one monkey (n=1) for the 7 dpi. To evaluate the viral loads for each monkey at the indicated time point, qRT-PCR were performed with two replicates. **b-d**, Histopathology and immunohistochemical examination of lung tissues from pre-exposure, post-exposure and control monkeys. One monkey from each group was euthanized and necropsied on 5 dpi. Samples for histological examination were stored in formalin for 7 days, embedded in paraffin, sectioned, and stained prior to examination by light microscopy. Hematoxylin and eosin sections exhibited the interstitial pneumonia and inflammatory factor infiltration in tissues. Masson's trichrome showed lung tissue fibrosis. Scale bar = 200 μm.

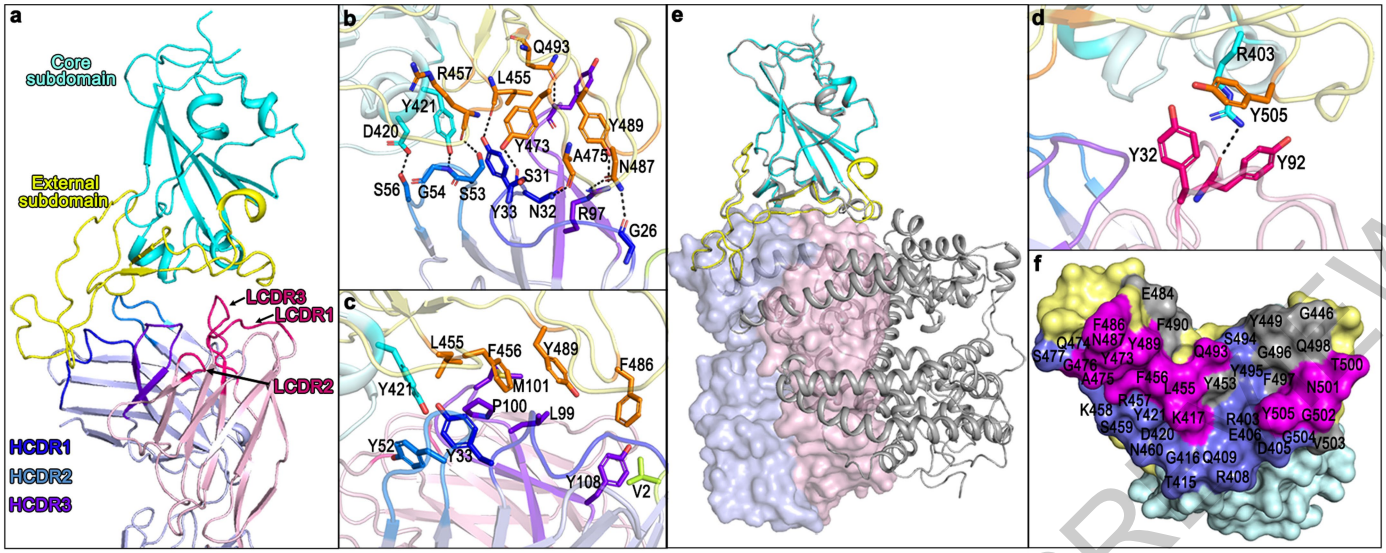

Fig. 4 | The crystal structure of CB6 and SARS-CoV-2-RBD complex and the competitive binding of CB6 and hACE2 with SARS-CoV-2-RBD. a, The complex structure of CB6 bound to SARS-CoV-2-RBD. The SARS-CoV-2-RBD is colored in cyan (core subdomain) and yellow (external subdomain). The variable fragment of CB6 is shown with HCDR1, HCDR2, and HCDR3 loops from the V_H domain (purple) colored in blue, marine and purple, while the LCDR1, LCDR2 and LCDR3 loop from the V_L domain (pink) are colored in hot-pink, respectively. **b-c**, Both hydrophilic interactions (b) and hydrophobic interactions (c) between CB6 heavy chain and SARS-CoV-2-RBD are displayed. **d**, The binding details between CB6 light chain and SARS-CoV-2-RBD are also presented. The hydrogen bonds are shown as dashed black lines. **e**, Superimposition of CB6/SARS-CoV-2-RBD complex and hACE2/SARS-CoV-2-RBD (PDB code: 6LZG) revealed the steric competition between CB6 and hACE2 for RBD binding. CB6/SARS-CoV-2-RBD structure was superimposed on hACE2/SARS-CoV-2-RBD to demonstrate steric hindrance. hACE2 is shown as cartoon (gray). **f**, Competitive binding surfaces of CB6 with hACE2 on SARS-CoV-2-RBD. The SARS-CoV-2-RBD binding surface to ACE2 and CB6 is shown. The residues bound by both CB6 and hACE2 are colored in magenta. The residues in contact with hACE2 alone are colored in gray while the residues in contact with CB6 alone are colored in blue. The amino acids on SARS-CoV-2-RBD interface contacting CB6 or ACE2 are labeled.

Methods

Study design

This study was designed to isolate SARS-CoV-2 specific MAbs from the blood of patients recovering from SARS-CoV-2 infection; characterize the properties of MAbs including blocking function, binding affinity, neutralization against SARS-CoV-2 and neutralizing mechanism; then test a best performing MAb for therapeutic efficacy in rhesus macaques.

PBMCs were isolated following the manufacturer's instructions (GE Healthcare) before being subjected to cell sorting as previously reported[17]. Briefly, PBMCs were incubated with His-tagged SARS-CoV-2-RBD at 100 nM before staining with anti-CD3, anti-CD16, anti-CD235a, anti-CD19, anti-CD38, anti-CD27 and anti-His. Antigen-specific memory B cells were identified by the following markers: $CD3^-$, $CD16^-$, $CD235a^-$, $CD38^-$, $CD19^+$, $CD27^+$, $hIgG^+$ and His^+, and sorted into 96-well PCR plates with single cell per well. Flow cytometric analysis and cell sorting were performed on a BD FACSAria III flow cytometer (BD Biosciences) and the data were analyzed using FlowJo. The genes encoding Ig V_H and V_L chains were amplified by 5'RACE and nested PCR. The variable regions of these genes were then linked with the coding sequences for human IgG1 constant region to generate full-length MAbs, which were then expressed and purified under good laboratory practice (GLP) conditions.

Eleven MAbs were generated with this method. Through blocking assays for SARS-CoV-2-RBD/hACE2 by FACS, two MAbs were analyzed for several properties: (a) binding specificity for MERS-CoV, SARS-CoV and SARS-CoV-2, (b) the competition assay for MAbs binding using Octet, and (c) ability of MAbs to neutralize the SARS-CoV-2 in Vero E6 cell. These results suggested that these two MAbs specifically bound and potently neutralized SARS-CoV-2 *in vitro*. Using a rhesus macaque model of SARS-CoV-2 infection, we tested the protective and curative efficacy of CB6. We equally divided the nine animals into per-exposure, post-exposure and negative control group. Viral loads from throat swabs were detected between three groups over a consecutive period of 7 days. The animals were euthanized and necropsied on 5 dpi to evaluate the therapeutic effect of CB6. Then, we investigated the neutralizing mechanism of the MAb through structural analysis of CB6/SARS-CoV-2-RBD. The high-resolution complex structure clarified that the binding surface of CB6 on SARS-CoV-2-RBD was overlapped with that of hACE2, indicating the substantial stereospecific hindrance to hACE2 contacting RBD.

Cells and Viruses

HEK293T (ATCC, CRL-3216) cells, Huh7 (Institute of Basic Medical Sciences CAMS, 3111C0001CCC000679) cells, Calu-3 (ATCC, HTB-55) cells and Vero E6 (ATCC, CRL-1586) cells were cultured at 37 °C in Dulbecco's Modified Eagle medium (DMEM) supplemented with 10% fetal bovine serum (FBS). SARS-CoV-2 named BetaCoV/Wuhan/IVDC-HB-envF13/2020 (Accession ID: EPI_ISL_408511) was isolated by National Institute for Virus Disease Control and Prevention, Chinese Center for Disease Control and Prevention. Vero E6 cells were applied to the reproduction of SARS-CoV-2 stocks.

Gene construction

Recombinant proteins SARS-CoV-2-RBD and hACE2 were used in assays of FACS, SPR, BLI and crystal screening. The coding sequences of SARS-CoV-2-RBD tagged with a C-terminal 6×His tag was cloned into the **pCAGGS** expression vector using the *Eco*RI and *Xho*I restriction sites. The coding sequences of ACE2 (residues 19-615, accession number: BAJ21180) was cloned into the baculovirus transfer vector **pFastbac1** (Invitrogen) containing an N-terminal gp67 signal peptide and a C-terminal 6×His tag. The full-length coding region of SARS-CoV S (accession number: NC_004718), MERS-CoV S (accession number: JX869050) and SARS-CoV-2 S protein with a C-terminal Flag tag was cloned into the **pCAGGS** vector using the *Eco*RI and *Sma*I restriction sites (**pCAGGS**-SARS-S-Flag, **pCAGGS**-MERS-S-Flag and **pCAGGS**-SARS-CoV-2-S-Flag). The **pEGFP-N1**-hACE2 plasmid was constructed by cloning the coding region of ACE2 into **pEGFP-N1** using restriction enzymes *Xho*I and *Sma*I.

Protein expression and purification

The SARS-CoV-2-RBD recombinant protein was expressed in HEK293T cells. The **pCAGGS** plasmid containing SARS-CoV-2-RBD coding sequences was transiently transfected into cells. After 3 days, the supernatant was collected and soluble protein was purified by Ni affinity chromatography using a HisTrap HP 5 mL column (GE Healthcare). The sample was further purified via gel filtration chromatography with a Superdex 200 column (GE Healthcare) in a buffer composed of 20 mM Tris-HCl (pH 8.0) and 150 mM NaCl. The Bac-to-Bac baculovirus expression system (Invitrogen) was used to express the hACE2 for Octet analysis. The constructed **pFastbac1** vectors were transformed into DH10Bac competent cells to generate recombinant bacmids. Transfection of bacmids and virus amplification were conducted in Sf9 cells, while Hi5 cells were used for protein expression. The soluble hACE2 protein was purified by the same process as above.

FACS assay

The activity of MAbs to block SARS-CoV-2-RBD and hACE2 binding was assessed by FACS. HEK293T cells were transiently transfected by **pEGFP-N1**-hACE2 expression plasmid for 24 hours. The SARS-CoV-2-RBD protein at a concentration of 200 ng/mL was mixed with MAbs or isotype IgG at a molar ratio of 1: 10 and incubated at 4°C for 1 hour. Then mixtures were added to 5×10^5 HEK293T cells expressing hACE2 and incubated at 4°C for another 1 h. After washing with PBS for three times, the cells were stained with anti-His/APC antibody for another 30 min and analyzed using flow cytometry (BD FACSCalibur).

To test the binding specificity, **pCAGGS**-SARS-S-Flag, **pCAGGS**-MERS-S-Flag and **pCAGGS**-SARS-CoV-2-S-Flag plasmids were transfected into HEK293T cells using PEI (Alfa) according to the manufacturer's instructions. 4×10^5 cells were collected 24 h after transfection, suspended in permeabilization solution (BD) on ice for 20 min. After washing with PBS twice, the cells were incubated with 20 μg/mL CA1, CB6, 80R, 4C2 or isotype IgG, respectively at room temperature for 1 h, followed by washing with PBS twice and further incubation with both anti-human IgG/APC (with the exception of 4C2, which used anti-mouse IgG/APC as the second antibody) and anti-Flag/FITC antibodies. After washing, the cells were analyzed using a BD FACSCalibur. All the above data were analyzed using FlowJo.

SPR

SPR measurements were done at room temperature using a BIAcore 8K system with Protein A biosensor chips (GE Healthcare). For all measurements, the buffer consisting of 150 mM NaCl, 10 mM HEPES, pH 7.4 and 0.005% (v/v) Tween-20 was used as running buffer, and all proteins were exchanged into this buffer in advance through gel filtration. The blank channel of the chip served as the negative control. Two MAbs were captured on the chip at 6000 response units. Gradient concentrations of SARS-CoV-2-RBD (from 50 nM to 3.125 nM with 2-fold dilution) were then flowed over the chip surface. After each cycle, the sensor was regenerated with Gly-HCl (pH1.7). The affinity was calculated using a 1:1 (Langmuir) binding fit model with BIAevaluation software.

BLI

The competitive binding of CA1, CB6 and hACE2 were measured by BLI using the Octet RED96 system (FortéBio). All experiments were performed at 25 °C in a buffer containing 50 mM Tris-HCl and 100 mM NaCl, pH7.0. Streptavidin biosensors were pre-equilibrated in the buffer for at least 10 min before use in experiments. Biotinylated SARS-CoV-2-RBD was loaded onto streptavidin biosensors for 300 s. For determining competitive characteristics, sensors were immersed with the first protein (or buffer as a control) for 240 s and then the second one for another 240 s. We analyzed the data using FortéBio Data Analysis.

Neutralization assay

SARS-CoV-2 pseudovirus preparation was performed as described[27]. Briefly, the plasmids of 15 μg **pCAGGS**-SARS-CoV-2-S and 15 μg **pNL4-3**. luc.RE were co-transfected into HEK293T cells. 48 h later, the supernatant was sequentially harvested, centrifuged and filtered through a 0.22 μm sterilized membrane. The $TCID_{50}$ was determined by the transduction of pseudovirus into Huh7 cells. For the neutralization assay, 10^4 cells/well in 100 μL were seeded in the 96-well plates 16 h before infection. 50 μL supernatant containing 10^3 $TCID_{50}$ pseudovirus was incubated with equal volume of 3-fold serially diluted antibodies for 1 h at 37 °C. Both MAbs were tested in the concentrations ranging from 5.08 ng/mL to 100 μg/mL in the context of Huh7 cells and Calu-3 cells. While for HEK293T, 15.24 ng/mL to 300 μg/mL were used. The mixtures of pseudoviruses and MAbs were then added to Huh7 cells with 2 replicates. After 4 h incubation, the medium was replaced with DMEM containing 10% fetal bovine serum, and the samples were incubated for an additional 24 h at 37 °C. Transfer cell lysates (50 μL/well) into luminometer plates (Microfluor 96-well plates). Add luciferase substrate (50 μL/well) included in luciferase assay system. Luciferase activity was measured using a GloMax 96 Microplate luminometer (Promega). The 50% neutralization dose was calculated using GraphPad Prism 6.0.

Infectious SARS-CoV-2 neutralization assay was performed. Vero E6 cells were seeded at 8×10^4 per well in a 24-well culture plates at 37 °C for 24 h before using. To reach an MOI at 0.005, 1 mL of diluted SARS-CoV-2 virus and 2-fold serially diluted CA1 (from 5.0 μg/mL to 0.15 μg/mL) or CB6 (from 1.0 μg/mL to 0.015 μg/mL) MAbs were mixed in the medium containing 2% FBS. Meanwhile, a control group (without antibody) was set up, and the culture supernatant containing virus was collected 30 h post infection. 140 μL of the supernatant at each well were taken and RNA extraction was carried out according to the instructions of QIAamp viral RNA mini kit. qRT-PCR detection was carried out with one-step TB Green PrimeScript PLUS RT-PCR Kit (Perfect Real Time), and the primer was RBD-qF1:5'- CAATGGTTTAACAGGCACAGG -3', RBD-qR1: 5′-CTCAAGTGTCTGTGGATCACG-3′. The total volume of the reaction system was 20 μL. The reaction conditions were: reverse transcription at 42°C for 5 min, pre-denaturation at 95°C for 10 s, 40 cycles including denaturation at 95°C for 10 s, annealing and extension at 60°C for 30 s. Another neutralization assay was based on CPE. Serial 2-fold dilutions of 50 μL of antibody CA1 (from 97.6 ng/mL to 200 μg/mL) or CB6 (from 48.8 ng/mL to 100 μg/mL) were prepared in a 96-well tissue culture plate in MEM medium. An equal volume of SARS-CoV-2 virus containing 100 $TCID_{50}$ was added, and the antibody-virus mixture was incubated at 37 °C for 1 h. The antibody-virus mixture was then transferred into a 96-well microtiter plate containing equal volume of confluent Vero E6 cells with 8 repeats and incubated at 37 °C for 3 days. Cells infected with 100 $TCID_{50}$ of SARS-CoV-2 and without the virus were applied as positive and uninfected controls, respectively. CPE in each well was observed daily and recorded on day 3 after infection. A virus back-titration was performed to assess the correct virus titer used in each experiment. The ND_{50} was calculated using GraphPad Prism 6.0. All experiments were followed the standard operating procedures of the approved Biosafety Level-3 facility.

Human samples

The human samples were obtained according to the procedures approved by the Chinese Academy of Sciences and complied with all relevant ethical regulations regarding human research. The blood was taken from a convalescent COVID-19 patient after she/he signed the informed consent form.

Animal experiments

All animal experiments were carried out according to the procedures approved by the Chinese Academy of Sciences and complied with all relevant ethical regulations regarding animal research.

Nine rhesus macaques (6-8 years old, three females and 6 males) were inoculated with 1×10^5 $TCID_{50}$ SARS-CoV-2 via intratracheal routes. The rhesus macaques were divided into 3 groups: control group (one female and two males), pre-exposure group (one female and two males) and post-exposure group (one female and two males). The rhesus macaques in control group were injected with PBS. The pre-exposure group were given 50 mg/kg antibody CB6 intravenously one day before viral challenge, while the post-exposure group were injected with the same amount of antibody on days 1 and 3 post exposure. In addition to routine clinical observation, oropharyngeal swabs were collected for 7 days. Swabs were placed into 1 mL of DMEM after collection. Viral RNAs were extracted by the QIAamp Viral RNA Mini Kit (Qiagen), according to the manufacturer's instructions and was eluted in 50 μL of elution buffer and used as the template for RT-PCR. The pairs of primers were used targeting S gene: RBD-qF1: 5′-CAATGGTTTAACAGGCACAGG-3′; RBD-qR1: 5′-CTCAAGTGTCTGTGGATCACG-3′. 2μL of RNA were used to verify the RNA quantity by HiScript® II One Step qRT-PCR SYBR® Green Kit (Vazyme Biotech Co., Ltd) according to the manufacturer's instructions. The amplification was performed as followed: 50°C for 3 min, 95°C for 30 s followed by 40 cycles consisting of 95°C for 10 s, 60°C for 30 s, and a default melting curve step in an ABI step-one machine.

Histopathology and Immunohistochemistry

Animal necropsies were performed according to a standard protocol. Samples for histological examination were stored in 10% neutral-buffered formalin for 7 days, embedded in paraffin, sectioned and stained with hematoxylin and eosin or Masson's trichrome prior to examination by light microscopy.

Crystal screening and structure determination

The SARS-CoV-2-RBD protein and CB6-Fab fragment were mixed at a molar ration of 1:1. The mixture was incubated on ice for 1 h and further purified by Superdex-200 column (GE Healthcare). 5 mg/mL and 10 mg/mL of SARS-CoV-2-RBD/CB6 proteins were used for crystal screening by vapour-diffusion sitting-drop method at 18 °C. Diffracting crystals were obtained in a concentration of 5 mg/mL at the mother liquid containing 24% w/v PEG 1500, 20% v/v glycerol.

Diffraction data were collected at Shanghai Synchrotron Radiation Facility (SSRF) BL17U1 (wavelength, 0.97919 Å) at 100K. For data collection, the crystals were cryo-protected by briefly soaking in reservoir solution supplemented with 20% (v/v) glycerol before flash-cooling in liquid nitrogen. The dataset was processed with XDS software (Wolfgang Kabsch). The complex structure of SARS-CoV-2-RBD/CB6 was determined by the molecular replacement method using Phaser[28] with our previously reported SARS-CoV-2 RBD structure (PDB code, 6LZG) and Fab structure (PDB code, 4TSA). The atomic models were completed with Coot[29] and refined with phenix.refine in Phenix[30], The Ramachandran plot determined by MolProbity indicates that 96.3% in most favored region, 3.53% in allowed region and 0.16% in disallowed region[31]. Data collection, processing, and refinement statistics are summarized in Extended Data Table 3. All structural figures were generated using Pymol software (http://www.pymol.org).

Sequence alignments

The GenBank accession number of the sequences used for analyzing the conservation of epitopes among SAR-CoV-2 are the following: MT263459, MT262993, MT262907, MT262915, MT262909, MT262916, MT262911, MT262908, MT262913, MT262912, MT262914, MT262906, MT262899, MT262898, MT262897, MT262904, MT262905, MT262896, MT262903, MT262902, MT262901, MT262900, MT262910, NC_045512, MT263396, MT263445, MT263421, MT258381, MT263391, MT263446, MT259269, MT263395, MT263468, MT263381, MT263074, MT258379, MT259271, MT263458, MT263429, MT258380, MT263382, MT259228, MT259227, MT259231, MT259226, MT259254, MT258377, MT259248, MT258383, MT263435, MT263398, MT258382, MT259277,

MT263392, MT263418, MT259236, MT263406, MT263417, MT263436, MT263443, MT259256, MT263452, MT259264, MT263420, MT259281, MT263450, MT263402, MT263433, MT263413, MT263404, MT259260, MT263437, MT263438, MT263403, MT263399, MT263464, MT259261, MT263439, MT259237, MT263410, MT259251, MT263444, MT263465, MT263447, MT263454, MT263463, MT263431, MT263424, MT263432, MT263416, MT259282, MT263419, MT263467, MT263440, MT263411, MT256917, MT256918, MT256924, MT263405, MT263408, MT263386, MT263469, MT263400, MT263425, MT263387, MT259285, MT263430, MT263449, MT263412, MT263414, MT263462, MT263434, MT263457, MT263461, MT263448, MT263423, MT263422, MT263415, MT259249, MT263442, MT259245, MT263427, MT263384, MT263441, MT263383, MT259243, MT263426, MT263388, MT263428, MT263455, MT263456, MT263453, MT263451, MT259235, MT263460, MT263390, MT263394, MT263466, MT259250, MT259280, MT259258, MT259239, MT259240, MT263407, MT263385, MT263397, MT263409, MT263393, MT263401, MT259279, MT259284, MT263389, MT259270, MT259259, MT259242 and MT259238. The sequence logos were generated using the web server of Weblogo (http://weblogo.berkeley.edu/logo.cgi).

Reporting summary

Further information on research design is available in the Nature Research Reporting Summary linked to this paper.

Data Availability

Further information and requests for resources and reagents should be directed to and will be fulfilled by the corresponding author Jinghua Yan (yanjh@im.ac.cn). are provided with this paper.

Code availability

The accession number for the atomic coordinates and diffraction data reported in this study is PDB code 7C01. The sequences of CA1 and CB6 MAbs have been deposited in GenBank with the accession codes MT470194- MT470197. are provided with this paper.

27. Du, L., Zhang, X., Liu, J. & Jiang, S. Protocol for recombinant RBD-based SARS vaccines: protein preparation, animal vaccination and neutralization detection. *Journal of visualized experiments : JoVE*, **2444**, https://doi.org/10.3791/2444 (2011).
28. McCoy, A. J. *et al*. Phaser crystallographic software. *Journal of applied crystallography* **40**, 658-674, https://doi.org/10.1107/S0021889807021206 (2007).
29. Emsley, P., Lohkamp, B., Scott, W. G. & Cowtan, K. Features and development of Coot. *Acta crystallographica Section D, Biological crystallography* **66**, 486-501, https://doi.org/10.1107/S0907444910007493 (2010).
30. Adams, P. D. *et al*. PHENIX: a comprehensive Python-based system for macromolecular structure solution. *Acta crystallographica Section D, Biological crystallography* **66**, 213-221, https://doi.org/10.1107/S0907444909052925 (2010).
31. Chen, V. B. *et al*. MolProbity: all-atom structure validation for macromolecular crystallography. *Acta crystallographica Section D, Biological crystallography* **66**, 12-21, https://doi.org/10.1107/S0907444909042073 (2010).

Acknowledgements We are grateful to S. Yao for his help to revise the manuscript. We thank the staff of beamline BL17U1 at the Shanghai Synchrotron Radiation Facility for assistance during data collection. We are grateful to Z. Fan (Institute of Microbiology, CAS) for her technical help on performing BLI and SPR. We thank all colleagues from National Biosafety Laboratory (Wuhan), CAS for their support during the study. We thank Y. Yao and Y. Peng from Wuhan Institute of Virology, CAS for supporting all the non-human primate experiment. We are grateful to F. Wang, Y. Hu, Y. Jia, S. Ren, L. Wu, and S. Tan for their help in performing the experiments. This work was supported by the Strategic Priority Research Program of CAS (XDB29040201), the National Major Science & Technology Major Project (2018ZX09711003), the National Key Research and Development Program of China (2020YFC0841400) and the National Natural Science Foundation of China (81922044 and 81973228). Q.W. is supported by the Youth Innovation Promotion Association CAS (Grant. 2018119). G.F.G and J.Y are supported by the foundation of the NSFC Innovative Research Group (grant no. 81621091).

Author contributions Q.W., G.F.G., and J.Y. initiated and coordinated the project. R.S., F.W., Q.W., G.F.G, Z.Y. and J.Y. designed the experiments. Q.W. performed the cell sorting with the help of Z.C. and J.S. R.S., X.D., T.S. and C.H. sequenced the antibodies. R.S. and X.D. conducted the SPR and Octet analysis. W.H. and L.W. prepared the pseudotype SARS-CoV-2 virus. T.S. evaluated the neutralizing potency using pseudovirus. Y.Z. and P.L. evaluated the neutralizing potency using authentic virus, with the help from B.Z., W.J.L. and G.W. C.S. conducted the animal experiments. Y.Z. and Z.Y. performed histopathology and immunohistochemistry assays with the assistance from G.G. and X.H.. X.D., X.B. and C.H. grew the complex crystals. J.Q. collected the diffraction data and determined the complex structure with the help from L.W. R.S., H.F., F.W.,G.F.G., Q.W. and J.Y. analyzed the data and wrote the manuscript.

Competing interests R. Shi, G.F. Gao, Q. Wang and J. Yan are listed as inventors on pending patent applications for MAb CA1 and CB6. The pending patent of CB6 has been licensed. The other authors declare that they have no competing interests.

Additional information

Supplementary information is available for this paper at https://doi.org/10.1038/s41586-020-2381-y.

Correspondence and requests for materials should be addressed to J.Y.

Reprints and permissions information is available at http://www.nature.com/reprints.

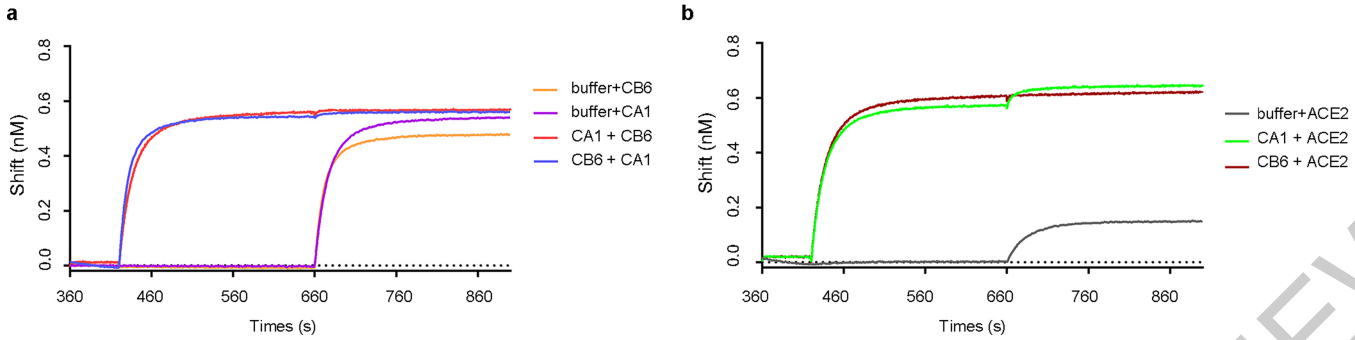

Extended Data Fig. 1 | Analysis of direct competitive binding characteristics of MAbs and hACE2. a-b, Competition between MAbs and hACE2 for binding to SARS-CoV-2-RBD. Octet sensors immobilized with SARS-CoV-2-RBD were first saturated with one MAb or the kinetic buffer and then exposed to the other MAb or hACE2 protein. The experiments were independently performed twice and similar results were obtained. The binding profiles of one experiment were shown.

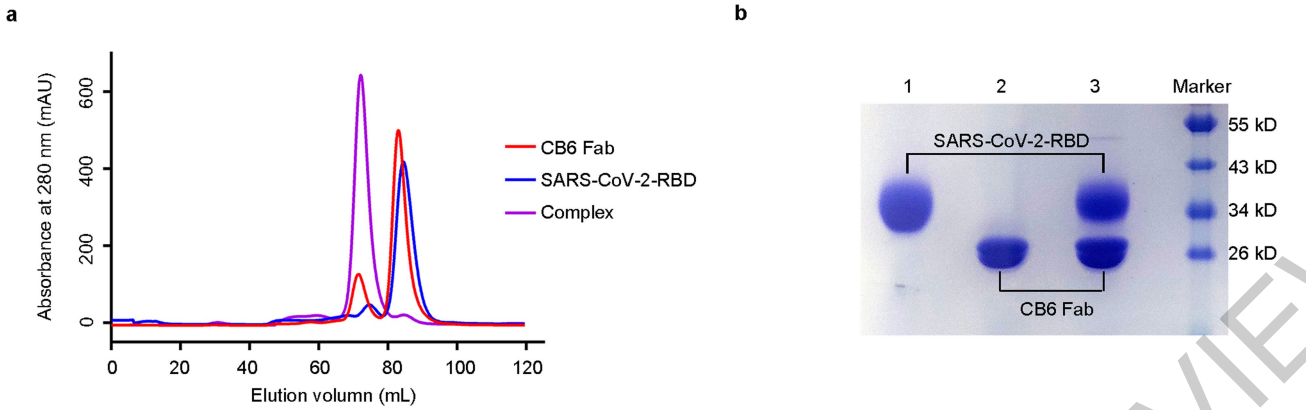

Extended Data Fig. 2 | Preparation complex protein of CB6-Fab/SARS-CoV-2-RBD. a, Gel filtration profiles of CB6-Fab (red), SARS-CoV-2-RBD (blue) and the complex (purple) were analyzed by size-exclusion chromatography as indicated. CB6-Fab forms stable complex with SARS-CoV-2-RBD. The experiments were independently performed twice and similar results were obtained. **b**, The SDS-PAGE analyses are shown in reducing (+DTT) conditions. CB6-Fab was de-polymerized into V_H and V_L fragments (25 kD). SARS-CoV-2-RBD exhibited a diffuse band due to glycosylation (38 kD). For gel source data, see Supplementary Figure 1.

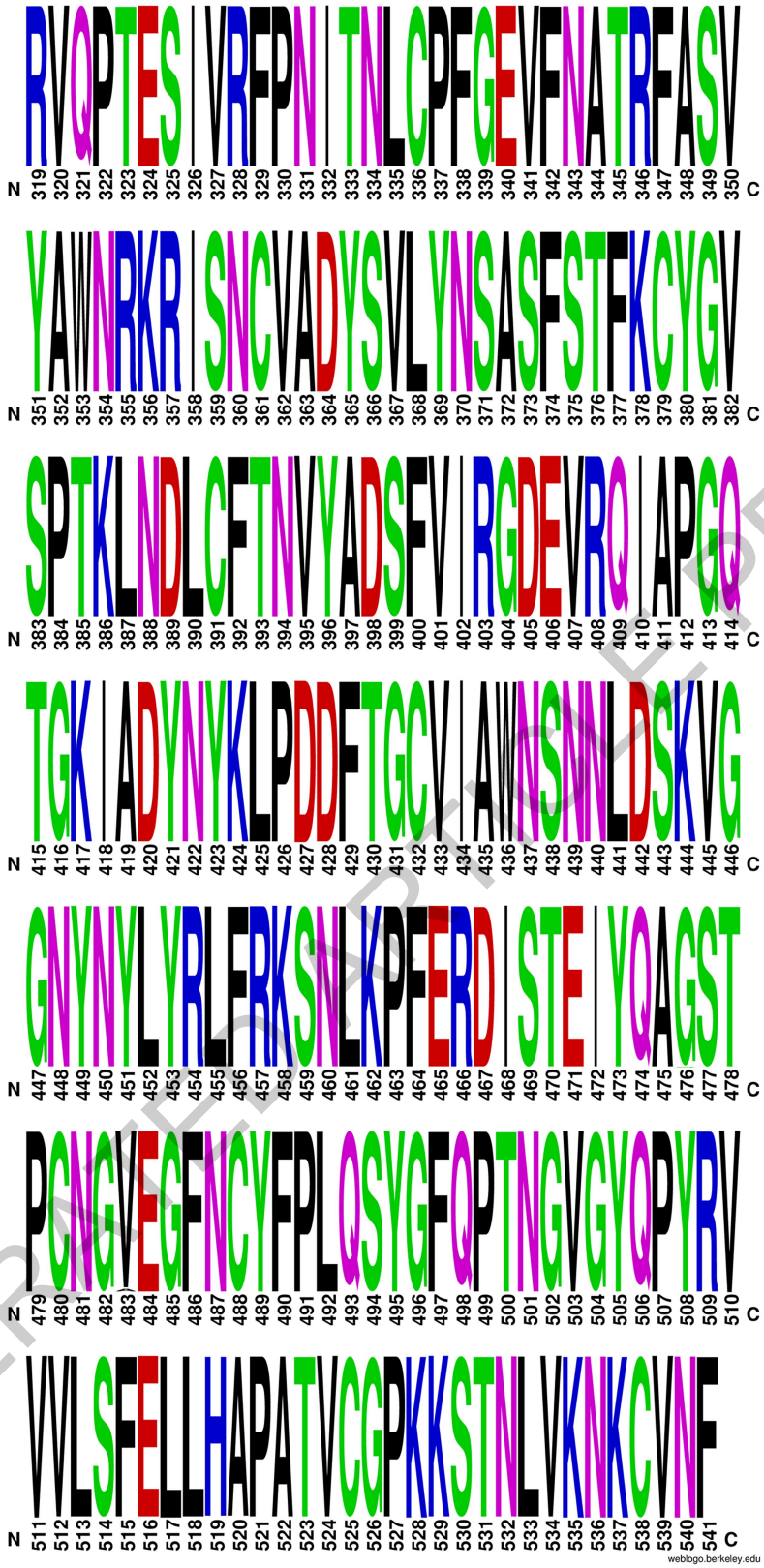

Extended Data Fig. 3 | Sequence alignment of RBD among SARS-CoV-2 strains. We obtained 157 full-length sequences of SARS-CoV-2-RBD by searching the NCBI databank. The sequence logos were generated using the web server of Weblogo (http://weblogo.berkeley.edu/logo.cgi). Four strains isolated from human patients in USA carries G476S and eight strains carries V483A (see materials and methods for details).

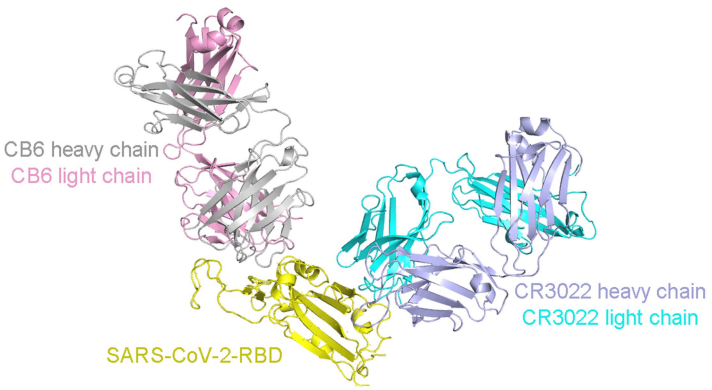

Extended Data Fig. 4 | Comparison of the CB6 and CR3022 binding epitopes. Superimposition of CB6/SARS-CoV-2-RBD and CR3022/SARS-CoV-2-RBD complex (PDB code: 6W41) reveals no epitope overlapping between CB6 and CR3022. SARS-CoV-2-RBD is shown as a cartoon (yellow). The CB6 heavy chain and light chain are colored in gray and pink, respectively. The CR3022 heavy chain and light chain are colored in cyan and light blue, respectively.

Extended Data Table 1 | Germline analysis of isolated MAbs specific for SARS-CoV-2

	V-H allele	D-H allele	J-H allele	Identity(V-H)	CDR3-H (aa)	V-L allele	J-L allele	Identity(V-L)	CDR3-L (aa)
CA1	IGHV1-18*01	IGHD2-15*01	IGHJ6*02	99.7%	AREGYCSGGSCYSGYYYYYGMDV	IGKV3-11*01	IGKJ3*01	98.2%	QQRRNWGT
CB6	IGHV3-66*01	IGHD3-10*02	IGHJ4*02	99.0%	ARVLPMYGDYLDY	IGKV1-39*01	IGKJ2*01	99.6%	QQSYSTPPEYT

V-(D)-J summary for the isolated MAbs. Listed are the top matches for Homo sapiens germline genes corresponding to the V, D and J of the heavy chain (V-H, J-H and D-H) and V and J of the light chain (V-L and J-L). CDR3-H and CDR3-L show the amino acid (aa) sequences of CDR3 for both chains.

Extended Data Table 2 | Binding characteristic of isolated MAbs specific for SARS-CoV-2

	Ka (1/Ms)	Kd (1/s)	K_D (M)
CA1	3.98E+06	1.16E-02	2.92E-09
	4.58E+05	3.15E-03	6.87E-09
	8.66E+05	3.69E-03	4.26E-09
CB6	8.95E+05	7.29E-04	8.15E-10
	2.32E+05	4.49E-04	1.93E-09
	4.72E+05	2.23E-04	4.73E-09

The binding characteristic for MAb CA1 and CB6. Listed are the results from three independent experiments. Ka indicates the binding rate of the indicated MAb with SARS-CoV-2-RBD. Kd is the dissociation rate. K_D signifies the affinity of the indicated MAb and the antigen.

Extended Data Table 3 | Data collection and refinement statistics

	CB6/SARS-CoV-2-RBD
Data collection	
Space group	P212121
Cell dimensions	
a, *b*, *c* (Å)	87.40, 106.73, 170.59
α, β, γ (°)	90.00, 90.00, 90.00
Resolution (Å)	50.00-2.88 (2.95-2.88) *
R_{sym} or R_{merge}	0.200 (1.596)
I / σI	12.2 (1.8)
Completeness (%)	99.9 (100.0)
Redundancy	13.0 (13.6)
Refinement	
Resolution (Å)	34.83-2.88
No. reflections	36767
R_{work} / R_{free}	0.2183/0.2663
No. atoms	
Protein	9670
Ligand/ion	0
Water	0
B-factors	
Protein	63.8
Ligand/ion	
Water	
R.m.s. deviations	
Bond lengths (Å)	0.003
Bond angles (°)	0.741

Diffraction data from one crystal were used for structure determination.
*Values in parentheses are for highest-resolution shell.

Extended Data Table 4 | Residues contributed interaction between CB6/SARS-CoV-2-RBD or hACE2/SARS-CoV-2-RBD

SARS-CoV-2-RBD	CB6	hACE2
R403	*Y92* * (12, 2 †), *T94* (3)	
D405	*Y92* (1), *T94* (7)	
E406	*T94* (4)	
R408	*T94* (4), *P95* (13)	
Q409	*T94* (2)	
T415	S56 (5), F58 (5)	
G416	Y52 (2), F58 (2)	
K417	Y33 (4), Y52 (7), D140 (4)	D30 (4, 1)
D420	Y52 (1), S56 (6)	
Y421	Y33 (6), Y52 (8), S53 (8, 2), G54 (7, 1), G55 (1)	
G446		Q42 (4)
Y449		D38 (9), Q42 (4, 1)
Y453		H34 (5, 1)
L455	Y33 (4, 1), P100 (10), M101 (5)	D30 (2), K31 (2), H34 (9)
F456	S31 (2), Y33 (3), S53 (1), P100 (8), M101 (2)	T27 (5), D30 (4), K31 (5)
R457	S53 (8), G54 (2, 1)	
K458	S31 (3), S53 (3), G54 (2)	
S459	G54 (1)	
N460	G54 (11), G55 (1), S56 (3, 1)	
Y473	S31 (13, 1), S53 (2)	T27 (1)
Q474	S31 (2)	
A475	F27 (3), T28 (8, 1), S31 (3), N32 (8, 1), R97 (1)	S19 (3), Q24 (4), T27 (2)
G476	F27 (2), T28 (5)	S19 (4), Q24 (5)
S477	T28 (2)	
E484		K31 (1)
F486	V2 (3), G26 (2), R97 (3), Y108 (7)	L79 (2), M82 (9), Y83 (11)
N487	G26 (4, 1), F27 (5), N32 (1), R97 (4, 1)	Q24 (15, 1), Y83 (8, 1)
Y489	R97 (3, 1), L99 (8), M101 (5)	T27 (7), F28 (7), K31 (6), Y 83 (1)
F490		K31 (2)
Q493	M101 (4), Y102 (6, 1)	K31 (3), H34 (6), E35 (11, 1)
Y495	*Y32* (1)	
G496		D38 (5), K353 (7, 1),
Q498		D38 (1), Y41 (8), Q42 (8, 1), L45 (3)
T500		Y41 (7, 1), L45 (1), N330 (8), D355 (8), R357 (3)
N501	*S30* (1)	Y41 (8, 1), K353 (11)
G502	*S28* (1), *Y92* (4)	K353 (4, 1), G354 (7), D355 (1)
G504	*Y92* (3)	
Y505	*S30* (4), *Y32* (13, 1), *Y92* (9, 1)	E37 (7), K353 (28), G354 (4), R393 (1)
	Total 321 ‡	Total 291

* Italic characters in the parentheses represent the residues from CB6 light chain CDRs.

† Numbers in the parentheses represent the number of hydrogen bonds between CB6 /SARS-CoV-2-RBD or hACE2/SARS-CoV-2-RBD residues which were analyzed by the Contact program in CCP4 suite (the distance cutoff is 3.5 Å).

‡ Numbers represent the number of van der Waals contacts between CB6 /SARS-CoV-2-RBD or hACE2/SARS-CoV-2-RBD residues, which were analyzed by the Contact program in CCP4 suite (the distance cutoff is 4.5Å).

nature research

Corresponding author(s): George Fu Gao

Last updated by author(s): May 16, 2020

Reporting Summary

Nature Research wishes to improve the reproducibility of the work that we publish. This form provides structure for consistency and transparency in reporting. For further information on Nature Research policies, see Authors & Referees and the Editorial Policy Checklist.

Statistics

For all statistical analyses, confirm that the following items are present in the figure legend, table legend, main text, or Methods section.

n/a	Confirmed	
☐	☒	The exact sample size (*n*) for each experimental group/condition, given as a discrete number and unit of measurement
☐	☒	A statement on whether measurements were taken from distinct samples or whether the same sample was measured repeatedly
☒	☐	The statistical test(s) used AND whether they are one- or two-sided *Only common tests should be described solely by name; describe more complex techniques in the Methods section.*
☒	☐	A description of all covariates tested
☒	☐	A description of any assumptions or corrections, such as tests of normality and adjustment for multiple comparisons
☐	☒	A full description of the statistical parameters including central tendency (e.g. means) or other basic estimates (e.g. regression coefficient) AND variation (e.g. standard deviation) or associated estimates of uncertainty (e.g. confidence intervals)
☒	☐	For null hypothesis testing, the test statistic (e.g. *F*, *t*, *r*) with confidence intervals, effect sizes, degrees of freedom and *P* value noted *Give P values as exact values whenever suitable.*
☒	☐	For Bayesian analysis, information on the choice of priors and Markov chain Monte Carlo settings
☒	☐	For hierarchical and complex designs, identification of the appropriate level for tests and full reporting of outcomes
☒	☐	Estimates of effect sizes (e.g. Cohen's *d*, Pearson's *r*), indicating how they were calculated

Our web collection on statistics for biologists contains articles on many of the points above.

Software and code

Policy information about availability of computer code

Data collection	BD FACSDiva Software 8.0.3, Biacore 8K Control Software 2.0.15.12933, GLOMAX 1.9.3, Octet Data Acquisition 9.0.0.26, UNICIORN 7.0.0.953 and XDS Program Package (Jan 31,2020).
Data analysis	FlowJo 7.6.1, Biacore Insight Evaluation 1.0.5.11069, GraphPad Prism 6.01, CCP4 7.0.072, Coot 0.8.9, Phenix 1.10.1-2155, Pymol 2.3.3 and ForteBio Data Analysis 9.0.0.10.

For manuscripts utilizing custom algorithms or software that are central to the research but not yet described in published literature, software must be made available to editors/reviewers. We strongly encourage code deposition in a community repository (e.g. GitHub). See the Nature Research guidelines for submitting code & software for further information.

Data

Policy information about availability of data

All manuscripts must include a data availability statement. This statement should provide the following information, where applicable:

- Accession codes, unique identifiers, or web links for publicly available datasets
- A list of figures that have associated raw data
- A description of any restrictions on data availability

The accession number for the atomic coordinates and diffraction data reported in this study is PDB code 7C01. The sequences of CA1 and CB6 MAbs have been deposited in GenBank with the accession codes MT470194- MT470197.

☒ Life sciences ☐ Behavioural & social sciences ☐ Ecological, evolutionary & environmental sciences Please select the one below that is

For a reference copy of the document with all sections, see nature.com/documents/nr-reporting-summary-flat.pdf

Life sciences study design

All studies must disclose on these points even when the disclosure is negative.

Sample size	No statistical methods were used to predetermine sample size. For the animal study, there are three groups investigated, including the control group without administration of MAbs (n=3), prophylactic group (n=3) and treatment group (n=3). The numbers of monkeys in each group meet the requirement for statistical analysis (at least 3 for each group), which is sufficient given the excellent technical reproducibility.
Data exclusions	No data were excluded.
Replication	The NHP experiments were not repeated in BSL-3 lab.
Randomization	We divided nine monkeys (three females and six males) into three groups, inluding the control group, the prophylactic group and the treatment group. Monkeys of the same sex were randomly divided into three groups.
Blinding	The investigators were not blinded to allocation during experiments and outcome assessment. Data collection and analysis were performed by different people, the sample classification were replaced by simple marks during data analysis.

Behavioural & social sciences study design

All studies must disclose on these points even when the disclosure is negative.

Study description	*Briefly describe the study type including whether data are quantitative, qualitative, or mixed-methods (e.g. qualitative cross-sectional, quantitative experimental, mixed-methods case study).*
Research sample	*State the research sample (e.g. Harvard university undergraduates, villagers in rural India) and provide relevant demographic information (e.g. age, sex) and indicate whether the sample is representative. Provide a rationale for the study sample chosen. For studies involving existing datasets, please describe the dataset and source.*
Sampling strategy	*Describe the sampling procedure (e.g. random, snowball, stratified, convenience). Describe the statistical methods that were used to predetermine sample size OR if no sample-size calculation was performed, describe how sample sizes were chosen and provide a rationale for why these sample sizes are sufficient. For qualitative data, please indicate whether data saturation was considered, and what criteria were used to decide that no further sampling was needed.*
Data collection	*Provide details about the data collection procedure, including the instruments or devices used to record the data (e.g. pen and paper, computer, eye tracker, video or audio equipment) whether anyone was present besides the participant(s) and the researcher, and whether the researcher was blind to experimental condition and/or the study hypothesis during data collection.*
Timing	*Indicate the start and stop dates of data collection. If there is a gap between collection periods, state the dates for each sample cohort.*
Data exclusions	*If no data were excluded from the analyses, state so OR if data were excluded, provide the exact number of exclusions and the rationale behind them, indicating whether exclusion criteria were pre-established.*
Non-participation	*State how many participants dropped out/declined participation and the reason(s) given OR provide response rate OR state that no participants dropped out/declined participation.*
Randomization	*If participants were not allocated into experimental groups, state so OR describe how participants were allocated to groups, and if allocation was not random, describe how covariates were controlled.*

All studies must disclose on these points even when the disclosure is negative.

Study description	*Briefly describe the study. For quantitative data include treatment factors and interactions, design structure (e.g. factorial, nested,*

Ecological, evolutionary & environmental sciences study design

hierarchical), nature and number of experimental units and replicates.

Research sample	*Describe the research sample (e.g. a group of tagged Passer domesticus, all Stenocereus thurberi within Organ Pipe Cactus National Monument), and provide a rationale for the sample choice. When relevant, describe the organism taxa, source, sex, age range and any manipulations. State what population the sample is meant to represent when applicable. For studies involving existing datasets, describe the data and its source.*
Sampling strategy	*Note the sampling procedure. Describe the statistical methods that were used to predetermine sample size OR if no sample-size calculation was performed, describe how sample sizes were chosen and provide a rationale for why these sample sizes are sufficient.*
Data collection	*Describe the data collection procedure, including who recorded the data and how.*
Timing and spatial scale	*Indicate the start and stop dates of data collection, noting the frequency and periodicity of sampling and providing a rationale for these choices. If there is a gap between collection periods, state the dates for each sample cohort. Specify the spatial scale from which the data are taken*
Data exclusions	*If no data were excluded from the analyses, state so OR if data were excluded, describe the exclusions and the rationale behind them, indicating whether exclusion criteria were pre-established.*
Reproducibility	*Describe the measures taken to verify the reproducibility of experimental findings. For each experiment, note whether any attempts to repeat the experiment failed OR state that all attempts to repeat the experiment were successful.*
Randomization	*Describe how samples/organisms/participants were allocated into groups. If allocation was not random, describe how covariates were controlled. If this is not relevant to your study, explain why.*
Blinding	*Describe the extent of blinding used during data acquisition and analysis. If blinding was not possible, describe why OR explain why blinding was not relevant to your study.*

Did the study involve field work? ☐ Yes ☐ No

Field work, collection and transport

Field conditions	*Describe the study conditions for field work, providing relevant parameters (e.g. temperature, rainfall).*
Location	*State the location of the sampling or experiment, providing relevant parameters (e.g. latitude and longitude, elevation, water depth).*
Access and import/export	*Describe the efforts you have made to access habitats and to collect and import/export your samples in a responsible manner and in compliance with local, national and international laws, noting any permits that were obtained (give the name of the issuing authority, the date of issue, and any identifying information).*
Disturbance	*Describe any disturbance caused by the study and how it was minimized.*

Reporting for specific materials, systems and methods

We require information from authors about some types of materials, experimental systems and methods used in many studies. Here, indicate whether each material, system or method listed is relevant to your study. If you are not sure if a list item applies to your research, read the appropriate section before selecting a response.

Materials & experimental systems

n/a	Involved in the study
☐	☒ Antibodies
☐	☒ Eukaryotic cell lines
☒	☐ Palaeontology
☐	☒ Animals and other organisms
☐	☒ Human research participants
☒	☐ Clinical data

Methods

n/a	Involved in the study
☒	☐ ChIP-seq
☐	☒ Flow cytometry
☒	☐ MRI-based neuroimaging

Antibodies

Antibodies used	anti-His/PE: Miltenyi Biotec, Cat No: 130-120-718, Clone No. GG11-8F3.5.1, Lot No. 5200110309, Dilution: 1:10; anti-hCD3/PE-Cy™5: BD Pharmingen™, Cat No: 555334, Clone No. UCHT1, Lot No. 7037531, Dilution: 1:20; anti-hCD16/PE-Cy™5: BD Pharmingen™, Cat No: 555408, Clone No. 3G8, Lot No. 7045714, Dilution: 1:20;

anti-hCD19/APC-Cy™7: BD Pharmingen™, Cat No: 557791, Clone No. SJ25C1, Lot No. 7118676, Dilution: 1:20;
anti-hCD27/Pacific Blue™: BioLegend, Cat No: 302821, Clone No. O323, Lot No. B223941, Dilution: 1:50;
anti-hCD38/APC: BD Pharmingen™, Cat No: 555462, Clone No. HIT2, Lot No. 7125887, Dilution: 1:20;
anti-CD235a/PE-Cy™5: BD Pharmingen™, Cat No: 559944, Clone No. GA-R2, Lot No. 7012580, Dilution: 1:20;
anti-hIgG/FITC: BD Pharmingen™, Cat No: 555786, Clone No. G18-145, Lot No. 6363638, Dilution: 1:20;
anti-hIgG/APC: BioLegend, Cat No: 409306, Clone No. HP6017, Lot No. B265810, Dilution: 1:100.
Anti-mIgG/APC: BD Pharmingen™, Cat No: 550874, Clone No. X56, Lot No. 7128657, Dilution: 1:100.

Validation

We follow the manufactures's instruction to use the above listed antibodies to stain human PBMCs. All antibodies work well.
anti-His/PE: (Miltenyi Biotec; Mouse; specific for His tag; applicable for Flow cytometry/Cell sorting [FC/FACS])
https://www.citeab.com/antibodies/7058497-130-120-718-anti-his-pe?des=d6e817455032c7cc

anti-hCD3/PE-Cy™5: (BD Pharmingen™; Mouse BALB/c IgG1, κ; specific for Human [QC Testing] CD3; applicable for flow cytometry [Routinely Tested]; 20 µL/test)
https://www.bdbiosciences.com/us/applications/research/t-cell-immunology/th-1-cells/surface-markers/human/pe-cy5-mouse-anti-human-cd3-ucht1-also-known-as-ucht-1-ucht-1/p/555334

anti-hCD16/PE-Cy™5: (BD Pharmingen™; Mouse BALB/c x DBA/2, also known as CD2F1 or CDF1 IgG1, κ; specific for Human [QC Testing], Rhesus, Cynomolgus, Baboon [Tested in Development] CD16; applicable for Flow cytometry [Routinely Tested]; 20 µL/test).
https://www.bdbiosciences.com/us/applications/research/stem-cell-research/cancer-research/human/pe-cy5-mouse-anti-human-cd16-3g8/p/555408

anti-hCD19/APC-Cy™7: (BD Pharmingen™, Mouse BALB/c IgG1, κ; specific for Human [QC Testing] CD19; applicable for flow cytometry [Routinely Tested], 5 µL/test)
https://www.bdbiosciences.com/us/applications/research/clinical-research/oncology-research/blood-cell-disorders/surface-markers/human/apc-cy7-mouse-anti-human-cd19-sj25c1-also-known-as-sj25-c1/p/557791

anti-hCD27/Pacific Blue™: (BioLegend, Mouse IgG1, κ; specific for Human, African Green, Baboon, Cynomolgus, Rhesus, Squirrel Monkey CD27; applicable for flow cytometry [Quality tested], 5 µL/test)
https://www.biolegend.com/en-us/products/pacific-blue-anti-human-cd27-antibody-6442

anti-hCD38/APC: (BD Pharmingen™, Mouse BALB/c IgG1, κ; specific for Human [QC Testing] CD19; applicable for flow cytometry [Routinely Tested], 20 µL/test)
https://www.bdbiosciences.com/us/applications/research/t-cell-immunology/regulatory-t-cells/surface-markers/human/apc-mouse-anti-human-cd38-hit2/p/555462

anti-CD235a/PE-Cy™5: (BD Pharmingen™, Mouse IgG2b, κ; specific for Human [QC Testing] CD19; applicable for flow cytometry [Routinely Tested])
https://www.bdbiosciences.com/us/reagents/research/antibodies-buffers/immunology-reagents/anti-human-antibodies/cell-surface-antigens/pe-cy5-mouse-anti-human-cd235a-ga-r2-hir2/p/559944

Eukaryotic cell lines

Policy information about cell lines

Cell line source(s)

HEK293T cells: ATCC, CRL-3216;
Huh7 cells: Institute of Basic Medical Sciences CAMS, 3111C0001CCC000679;
Calu-3 cells: ATCC, HTB-55;
Vero E6 cells: ATCC, CRL-1586.

Authentication

The cell lines were not authenticated since they were purchased commercially and are not commonly misidentified.

Mycoplasma contamination

The cells were not tested for mycoplasma contamination.

Commonly misidentified lines
(See ICLAC register)

The cell lines used in this study do not appear on the ICLAC register.

Palaeontology

Specimen provenance

Provide provenance information for specimens and describe permits that were obtained for the work (including the name of the issuing authority, the date of issue, and any identifying information).

Specimen deposition

Indicate where the specimens have been deposited to permit free access by other researchers.

Dating methods

If new dates are provided, describe how they were obtained (e.g. collection, storage, sample pretreatment and measurement), where they were obtained (i.e. lab name), the calibration program and the protocol for quality assurance OR state that no new dates are provided.

☐ Tick this box to confirm that the raw and calibrated dates are available in the paper or in Supplementary Information.

Animals and other organisms

Policy information about studies involving animals; ARRIVE guidelines recommended for reporting animal research

Laboratory animals	Nine Rhesus macaques (6-8 years old).
Wild animals	The study did not involve wild animals.
Field-collected samples	The study did not involve samples collected from the field.
Ethics oversight	Chinese Academy of Sciences

Note that full information on the approval of the study protocol must also be provided in the manuscript.

Human research participants

Policy information about studies involving human research participants

Population characteristics	We used the blood from one convalescent COVID-19 patient (female, 33 years old) in China.
Recruitment	The patient agreed to provide the biospecimen for detection, further diagnostic and scientific research when hospitalization.
Ethics oversight	Chinese Academy of Sciences

Note that full information on the approval of the study protocol must also be provided in the manuscript.

Clinical data

Policy information about clinical studies

All manuscripts should comply with the ICMJE guidelines for publication of clinical research and a completed CONSORT checklist must be included with all submissions.

Clinical trial registration	*Provide the trial registration number from ClinicalTrials.gov or an equivalent agency.*
Study protocol	*Note where the full trial protocol can be accessed OR if not available, explain why.*
Data collection	*Describe the settings and locales of data collection, noting the time periods of recruitment and data collection.*
Outcomes	*Describe how you pre-defined primary and secondary outcome measures and how you assessed these measures.*

ChIP-seq

Data deposition

☐ Confirm that both raw and final processed data have been deposited in a public database such as GEO.

☐ Confirm that you have deposited or provided access to graph files (e.g. BED files) for the called peaks.

Data access links *May remain private before publication.*	*For "Initial submission" or "Revised version" documents, provide reviewer access links. For your "Final submission" document, provide a link to the deposited data.*
Files in database submission	*Provide a list of all files available in the database submission.*
Genome browser session (e.g. UCSC)	*Provide a link to an anonymized genome browser session for "Initial submission" and "Revised version" documents only, to enable peer review. Write "no longer applicable" for "Final submission" documents.*

Methodology

Replicates	*Describe the experimental replicates, specifying number, type and replicate agreement.*
Sequencing depth	*Describe the sequencing depth for each experiment, providing the total number of reads, uniquely mapped reads, length of reads and whether they were paired- or single-end.*
Antibodies	*Describe the antibodies used for the ChIP-seq experiments; as applicable, provide supplier name, catalog number, clone name, and lot number.*
Peak calling parameters	*Specify the command line program and parameters used for read mapping and peak calling, including the ChIP, control and index files used.*
Data quality	*Describe the methods used to ensure data quality in full detail, including how many peaks are at FDR 5% and above 5-fold enrichment.*

Software | *Describe the software used to collect and analyze the ChIP-seq data. For custom code that has been deposited into a community repository, provide accession details.*

Flow Cytometry

Plots

Confirm that:

☒ The axis labels state the marker and fluorochrome used (e.g. CD4-FITC).

☒ The axis scales are clearly visible. Include numbers along axes only for bottom left plot of group (a 'group' is an analysis of identical markers).

☒ All plots are contour plots with outliers or pseudocolor plots.

☒ A numerical value for number of cells or percentage (with statistics) is provided.

Methodology

Sample preparation	Sample preparation listed in Methods
Instrument	BD FACSAria II, BD FACSCalibur and BD FACSCanto II.
Software	FlowJo 7.6.1
Cell population abundance	After cell sorting, the collected cells were subjected for RT-PCR to determine the genes of the IgG. Thus, we did not test the relevant cell populations within post-sort fractions.
Gating strategy	For the isolation of antigen-specific memory B cells, we used the unstained PBMCs as control to gate cells.

☒ Tick this box to confirm that a figure exemplifying the gating strategy is provided in the Supplementary Information.

Magnetic resonance imaging

Experimental design

Design type	*Indicate task or resting state; event-related or block design.*
Design specifications	*Specify the number of blocks, trials or experimental units per session and/or subject, and specify the length of each trial or block (if trials are blocked) and interval between trials.*
Behavioral performance measures	*State number and/or type of variables recorded (e.g. correct button press, response time) and what statistics were used to establish that the subjects were performing the task as expected (e.g. mean, range, and/or standard deviation across subjects).*

Acquisition

Imaging type(s)	*Specify: functional, structural, diffusion, perfusion.*
Field strength	*Specify in Tesla*
Sequence & imaging parameters	*Specify the pulse sequence type (gradient echo, spin echo, etc.), imaging type (EPI, spiral, etc.), field of view, matrix size, slice thickness, orientation and TE/TR/flip angle.*
Area of acquisition	*State whether a whole brain scan was used OR define the area of acquisition, describing how the region was determined.*

Diffusion MRI ☐ Used ☐ Not used

Preprocessing

Preprocessing software	*Provide detail on software version and revision number and on specific parameters (model/functions, brain extraction, segmentation, smoothing kernel size, etc.).*
Normalization	*If data were normalized/standardized, describe the approach(es): specify linear or non-linear and define image types used for transformation OR indicate that data were not normalized and explain rationale for lack of normalization.*
Normalization template	*Describe the template used for normalization/transformation, specifying subject space or group standardized space (e.g. original Talairach, MNI305, ICBM152) OR indicate that the data were not normalized.*
Noise and artifact removal	*Describe your procedure(s) for artifact and structured noise removal, specifying motion parameters, tissue signals and physiological signals (heart rate, respiration).*

Volume censoring

Define your software and/or method and criteria for volume censoring, and state the extent of such censoring.

Statistical modeling & inference

Model type and settings

Specify type (mass univariate, multivariate, RSA, predictive, etc.) and describe essential details of the model at the first and second levels (e.g. fixed, random or mixed effects; drift or auto-correlation).

Effect(s) tested

Define precise effect in terms of the task or stimulus conditions instead of psychological concepts and indicate whether ANOVA or factorial designs were used.

Specify type of analysis: ☐ Whole brain ☐ ROI-based ☐ Both

Statistic type for inference
(See Eklund et al. 2016)

Specify voxel-wise or cluster-wise and report all relevant parameters for cluster-wise methods.

Correction

Describe the type of correction and how it is obtained for multiple comparisons (e.g. FWE, FDR, permutation or Monte Carlo).

Models & analysis

n/a	Involved in the study
☐	☐ Functional and/or effective connectivity
☐	☐ Graph analysis
☐	☐ Multivariate modeling or predictive analysis

Functional and/or effective connectivity

Report the measures of dependence used and the model details (e.g. Pearson correlation, partial correlation, mutual information).

Graph analysis

Report the dependent variable and connectivity measure, specifying weighted graph or binarized graph, subject- or group-level, and the global and/or node summaries used (e.g. clustering coefficient, efficiency, etc.).

Multivariate modeling and predictive analysis

Specify independent variables, features extraction and dimension reduction, model, training and evaluation metrics.